Supplementary Information (SI) for Nanoscale Horizons.

Supplementary Information for

Molecular recruitment and release using DNA host condensates

Heather Romero Mercieca[1], Diana McGrory[1,†], Brian Perlstein[3,†], Britney Castañeda-Camacho[5,†]
Wing Lam Yu[3], Taneeka Anand[5], Jillian L. Blatti[6], Elisa Franco[1,2,4,*], Mahdi Dizani[2,*]

[1]Department of Bioengineering, University of California at Los Angeles, Los Angeles, CA 90095

[2]Department of Mechanical and Aerospace Engineering, University of California, Los Angeles, Los Angeles, CA 90095

[3]Department of Molecular, Cell, and Developmental Biology, University of California, Los Angeles, Los Angeles, CA 90095

[4]Molecular Biology Institute, University of California at Los Angeles, Los Angeles, CA 90095

[5]Department of Ecology and Evolutionary Biology, University of California, Los Angeles, Los Angeles, CA 90095

[6]Department of Chemistry in the Division of Natural Sciences, Pasadena City College, Pasadena, CA 91106

†These authors contributed equally

*Corresponding authors: mdizani@ucla.edu, efranco@seas.ucla.edu

1. Supplementary figures

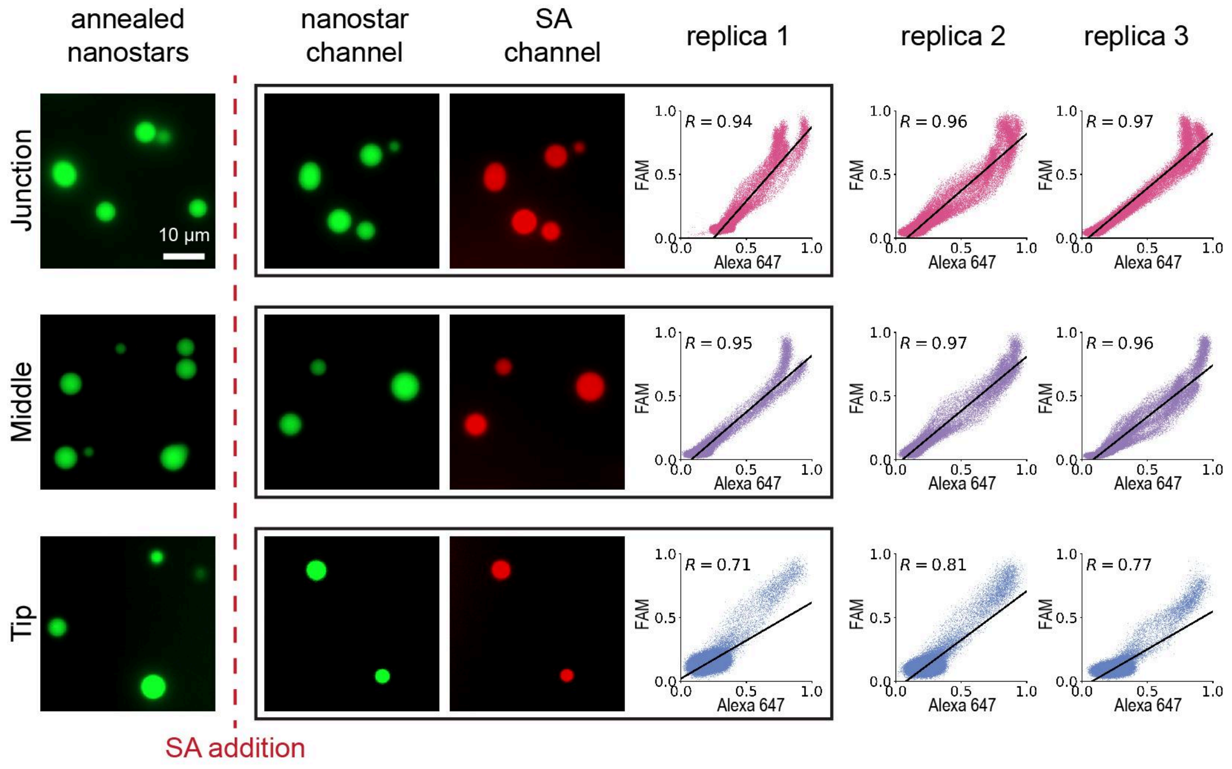

Figure S1. Colocalization analysis of SA with condensates. *Condensates were formed by annealing all the nanostar strands simultaneously (core plus the aptamer strands). Here streptavidin (SA) was added a few minutes after annealing. Epifluorescence imaging after SA addition was done within 5-10 minutes, showing rapid colocalization. The experiments were repeated three times using epifluorescence microscopy (n = 3).*

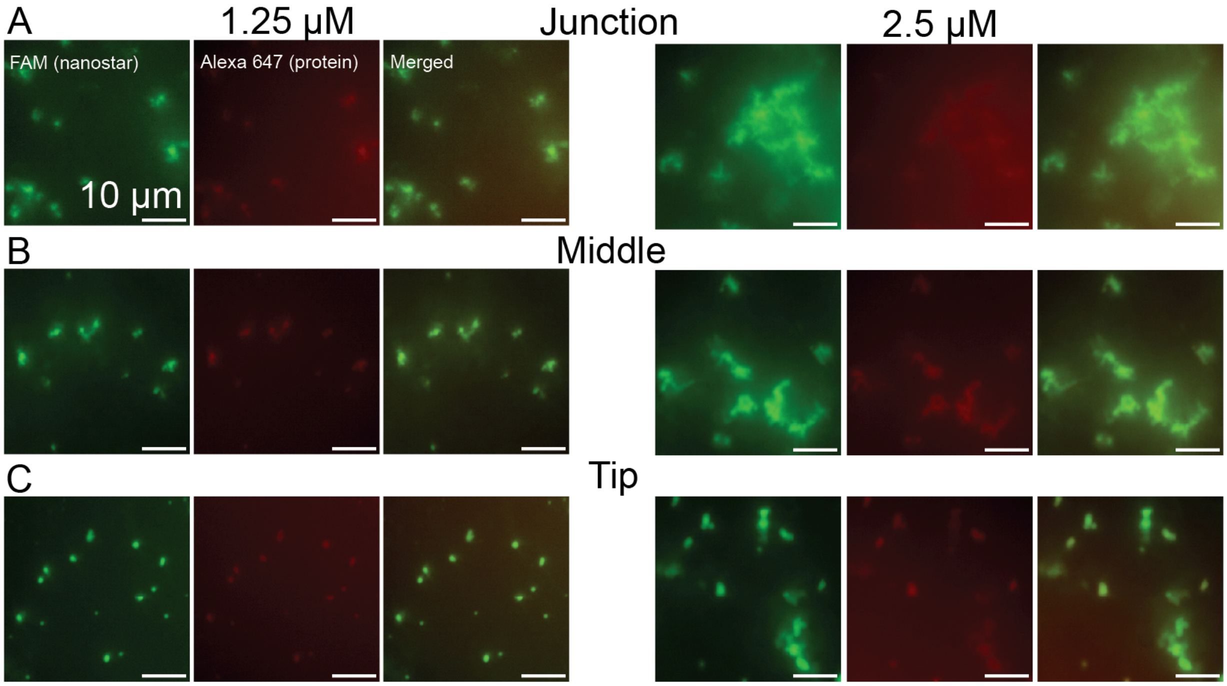

Figure S2. Concentration effect on nanostar condensation. *Example epifluorescence microscopy images for the nanostar variants in the presence of SA at 25 °C (60 minutes incubation) for (A) junction, (B) middle, and (C) tip designs.*

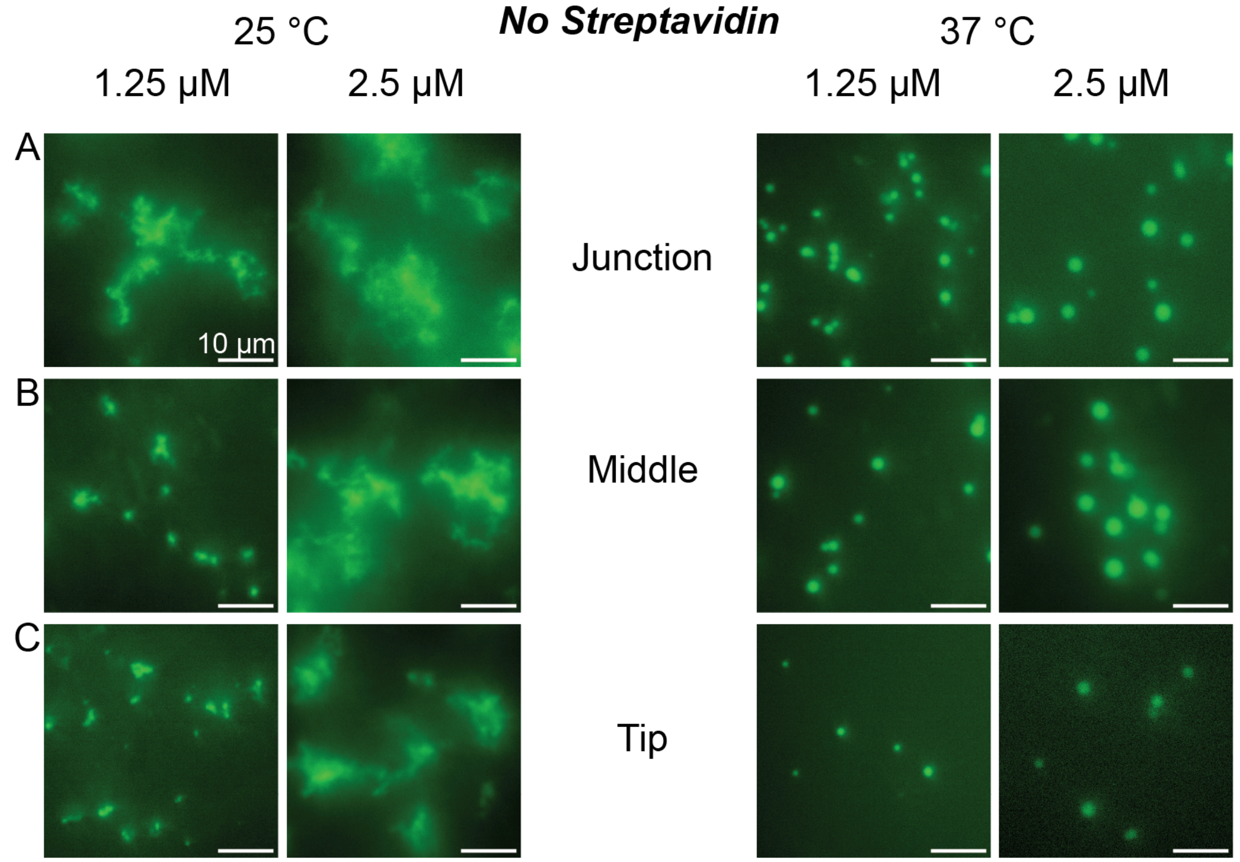

Figure S3. Temperature effect on condensates morphology. *Example condensate images for the nanostar variants without SA at 25 °C and 37 °C (60 minutes incubation) for (A) junction, (B) middle, and (C) tip designs. Images were taken using epifluorescence microscopy*

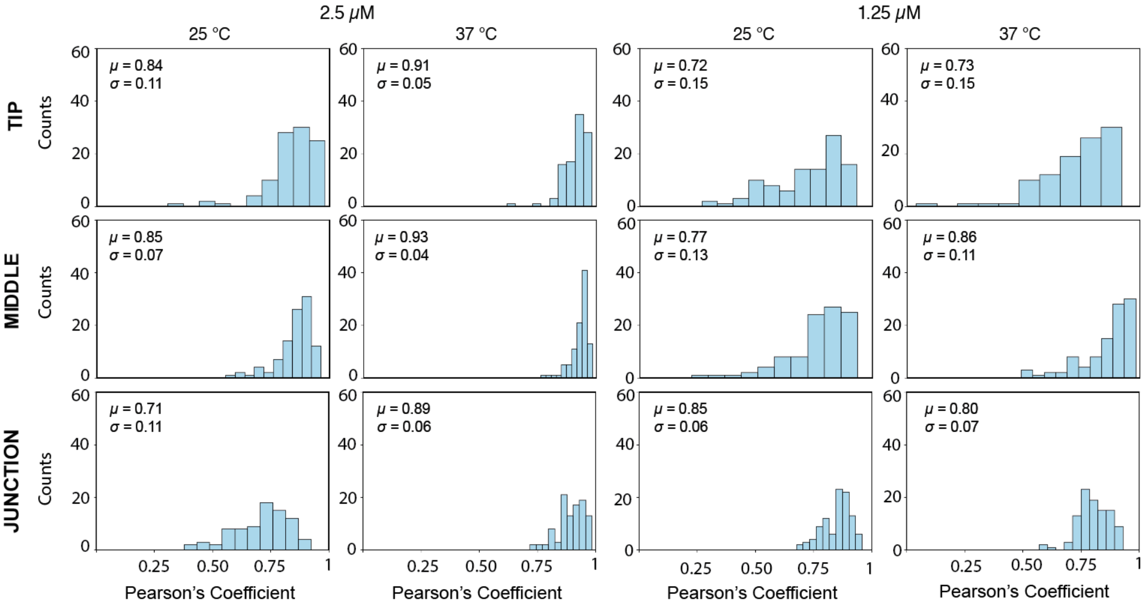

Figure S4. Colocalization analysis of SA and condensates. *Histograms showing the statistical distribution of Pearson's correlation coefficients (R) of 100 condensates (counts) after 60 minutes of incubation for junction, middle, and tip aptamer placements with SA. μ is the mean of R values, showing greater colocalization at 37 °C at the nanostar concentration of 2.5 μM. Standard deviation (σ) shows greater variability at 1.25 μM.*

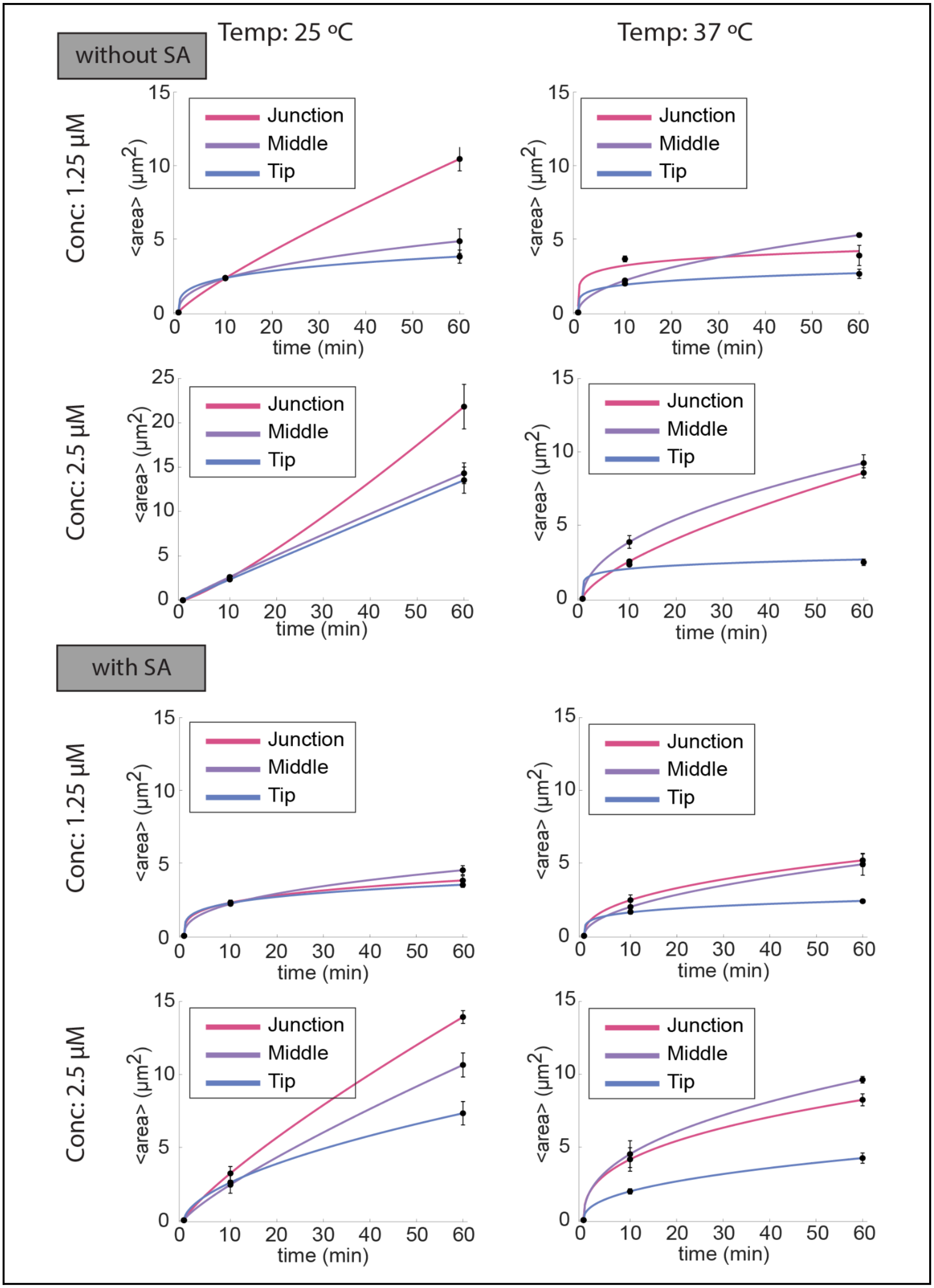
Temp: 25 ºC
Temp: 37 ºC
without SA
with SA
Conc: 1.25 μM
Conc: 2.5 μM
Conc: 1.25 μM
Conc: 2.5 μM
Junction
Middle
Tip
<area> (μm^2)
time (min)
0
5
10
15
20
25
10
20
30
40
50
60

Figure S5. Growth curves showing how temperature and concentration affect each design dynamics over 60 minutes. *Growth curves show the change in area (µm^2) over time (minutes) with and without SA. The curves are plotted at temperatures 25 °C and 37 °C, as well as across concentrations 1.25 µM and 2.5 µM. Curves with no SA show greater area growth for the junction design under 25 °C across both concentrations, and the middle design shows greater area growth under 37 °C across both concentrations. Meanwhile, the tip design shows consistently low area growth across temperature and concentration with no SA. Across all conditions, curves with SA depict the greatest area growth with the junction and middle designs, while the tip design consistently shows the least area growth. Dots represent the average of three experimental replicas (n = 3); error bars show the standard deviation of the mean. Curves were fitted to the following power law*[1]*:* $y = gt^{\alpha}$. *Corresponding growth curve parameters are listed in Tables S4 and S5.*

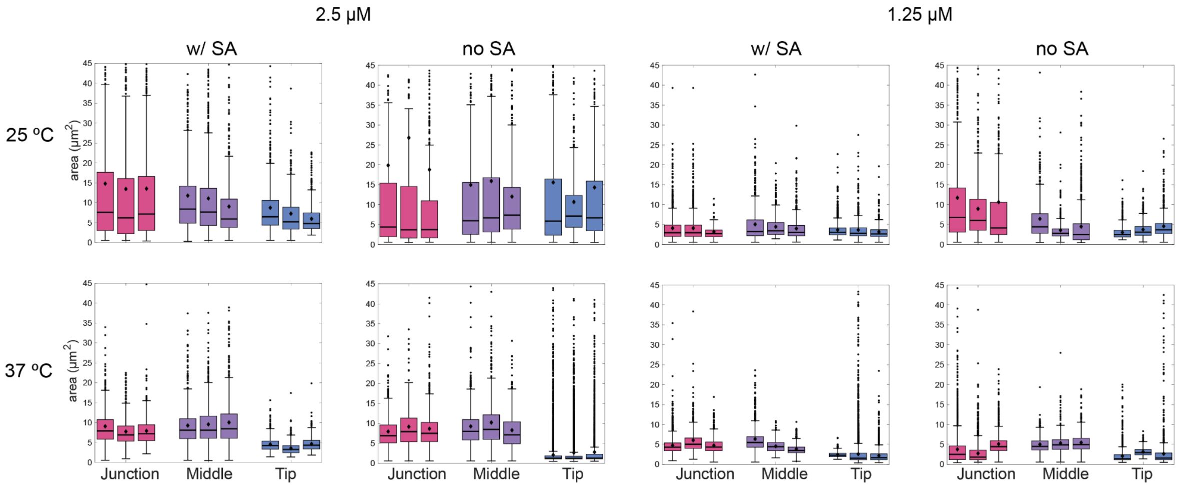

Figure S6. Box plots showing the distribution of condensate area distributions after 60 minutes at 25 °C and 37 °C among aptamer designs and concentrations. *Each concentration is plotted with SA added or without SA. Condensates at 25 °C at 2.5 µM are more consistent in area distribution across junction, middle and tip designs. The addition of SA at 1.25 µM resulted in a decrease in the condensate area.*

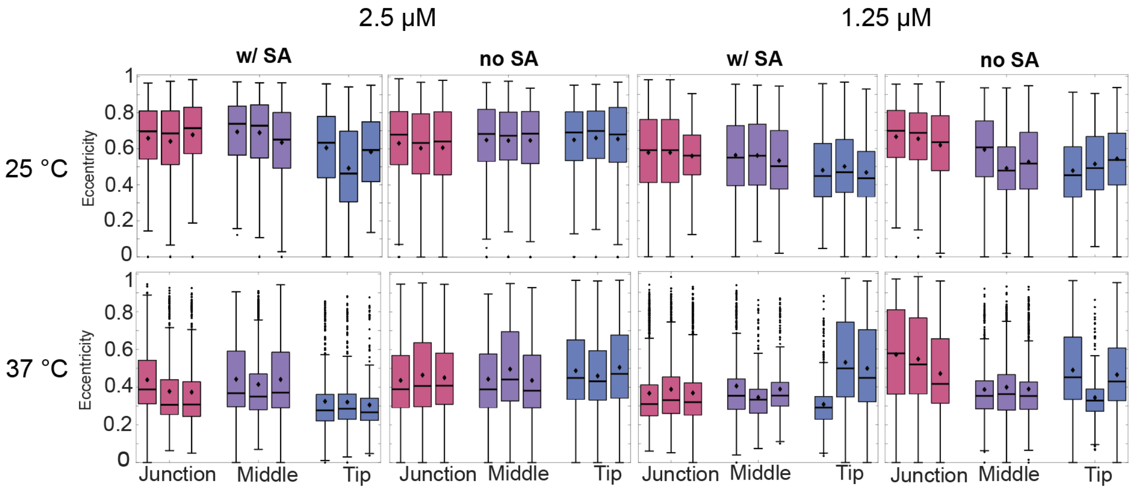

Figure S7. Box plots showing the eccentricity of DNA condensates formed using junction, middle, and tip nanostar designs at 25 °C and 37 °C after 60 minutes, in the presence and absence of SA, and at nanostar concentrations of 1.25 µM and 2.5 µM. *The addition of SA lowers eccentricity for junction and middle designs, consistent with the formation of more isotropic condensates. The tip design exhibits persistently low eccentricity across all conditions.*

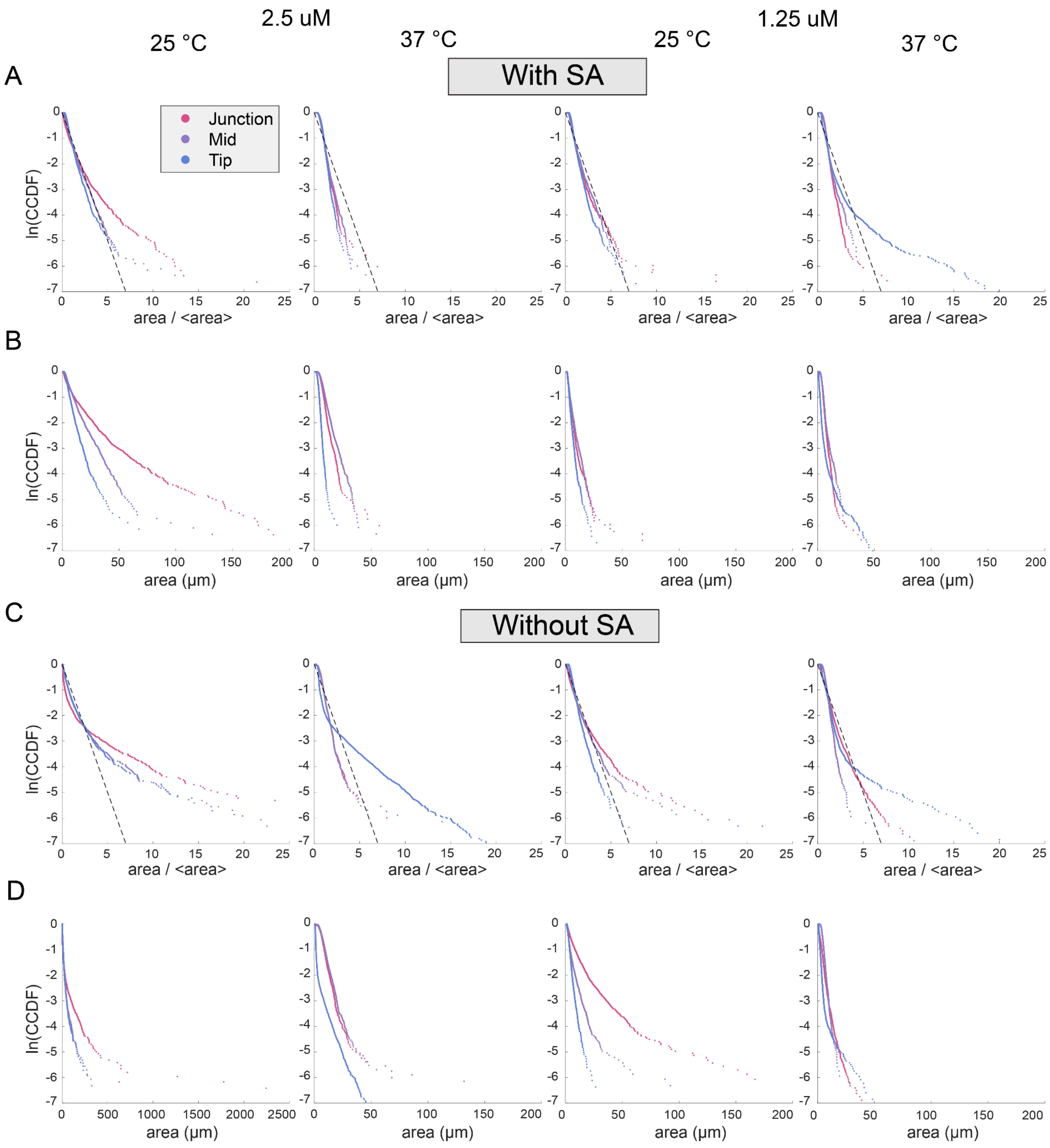

Figure S8. Complementary Cumulative Distribution Function (CCDF) plots showing the distribution of condensate sizes after 60 minutes across different aptamer designs and nanostar concentrations. *CCDF of condensate areas are plotted on a semi-log scale, revealing a negative slope for all aptamers across two different nanostar concentrations and temperatures. (A),(C) distributions are normalized with respect to the average condensate area. For comparison we include the CCDF of an exponential distribution also normalized with respect to its average, which is a line with slope -1 (black dashed lines). (B),(D) are non-normalized distributions. Triplicate data were pooled in a single dataset to generate these plots.*

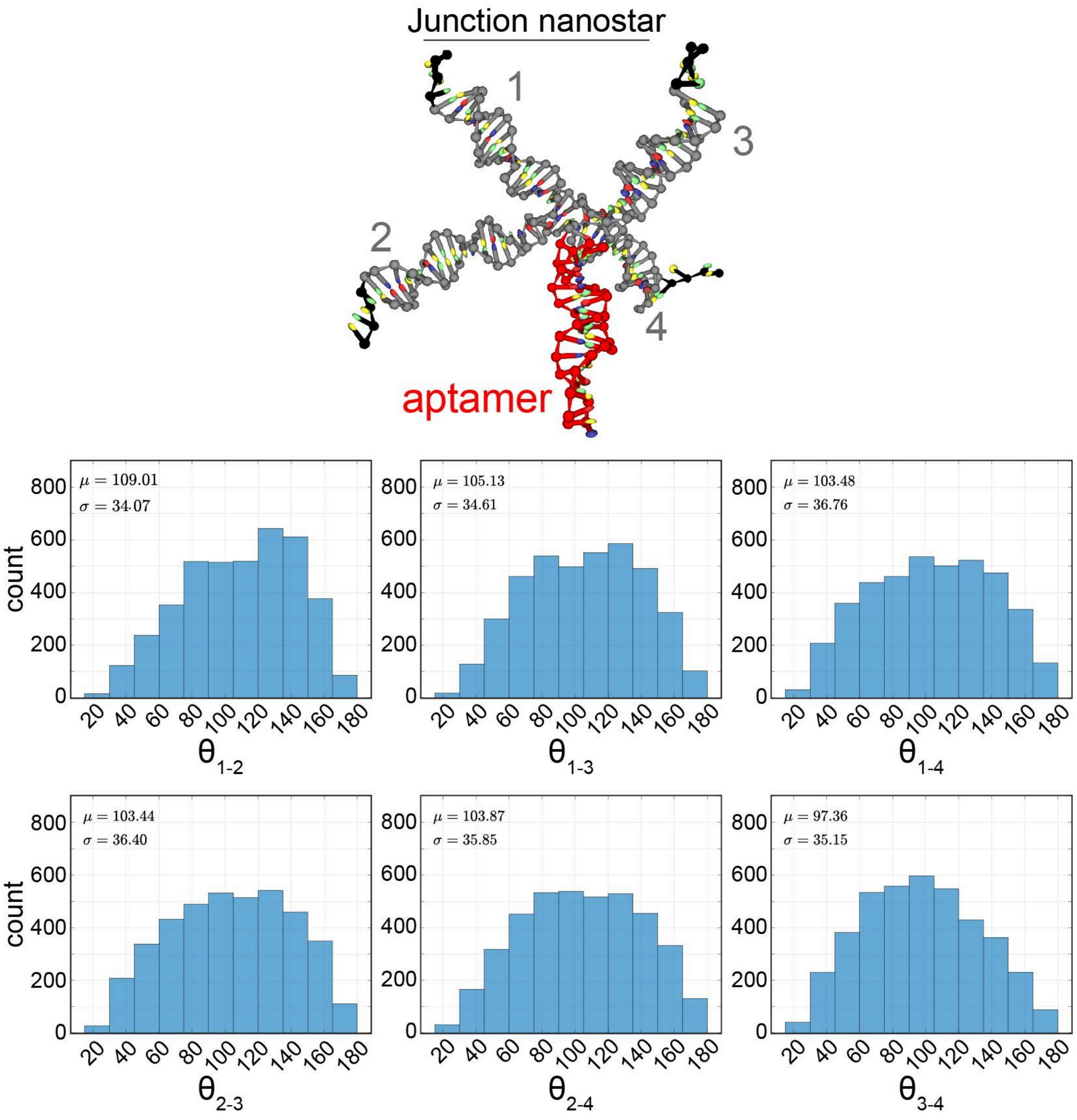

Figure S9. Angular distribution of the junction design. *Angular distributions of each and every pair of arms in the junction design. The i and j indices refer to the arm labels shown in the oxView representation (top).*

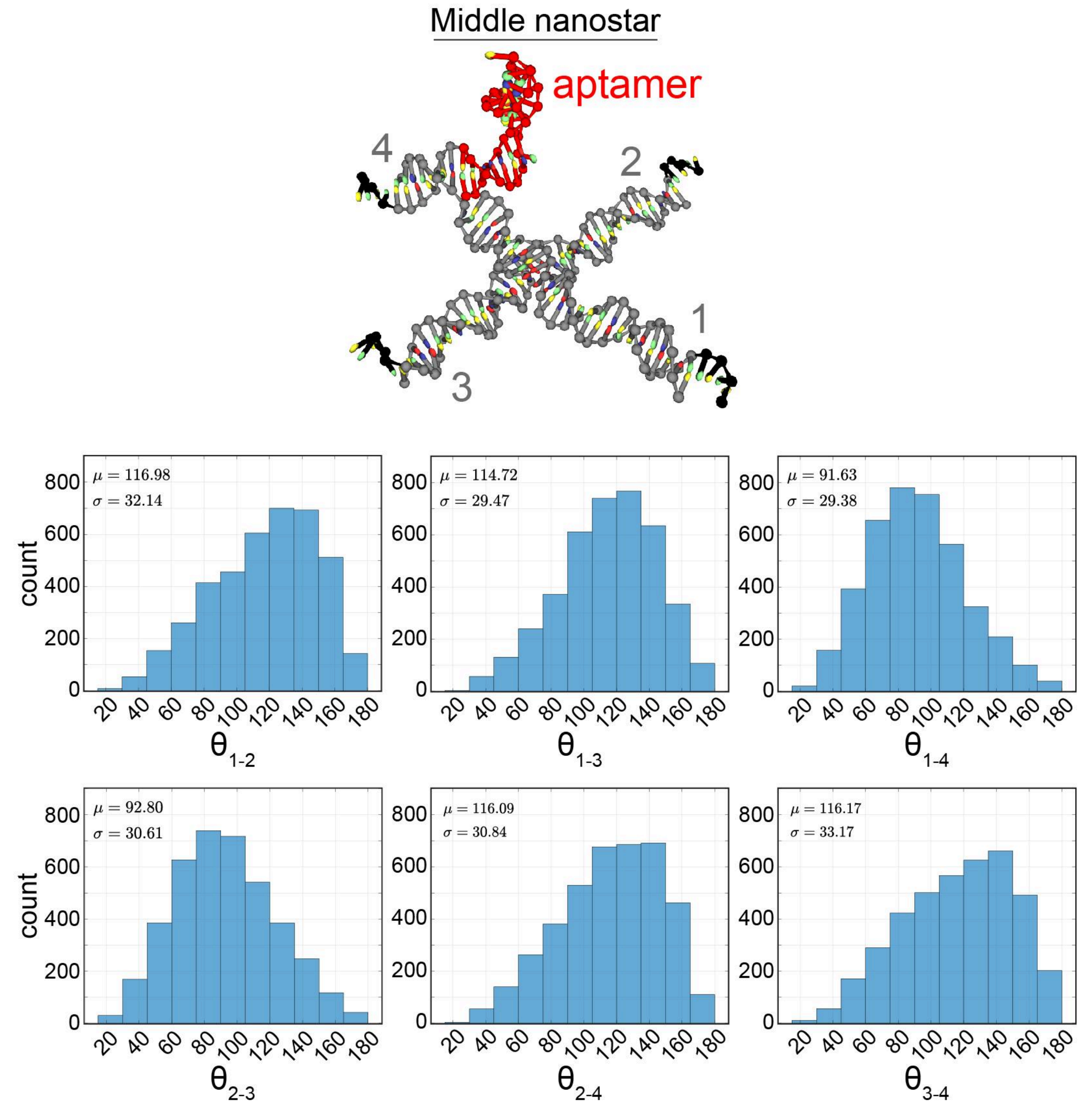

Figure S10. Angular distribution of the middle design. *Angular distributions of each and every pair of arms in the middle design. The i and j indices refer to the arm labels shown in the oxView representation (top).*

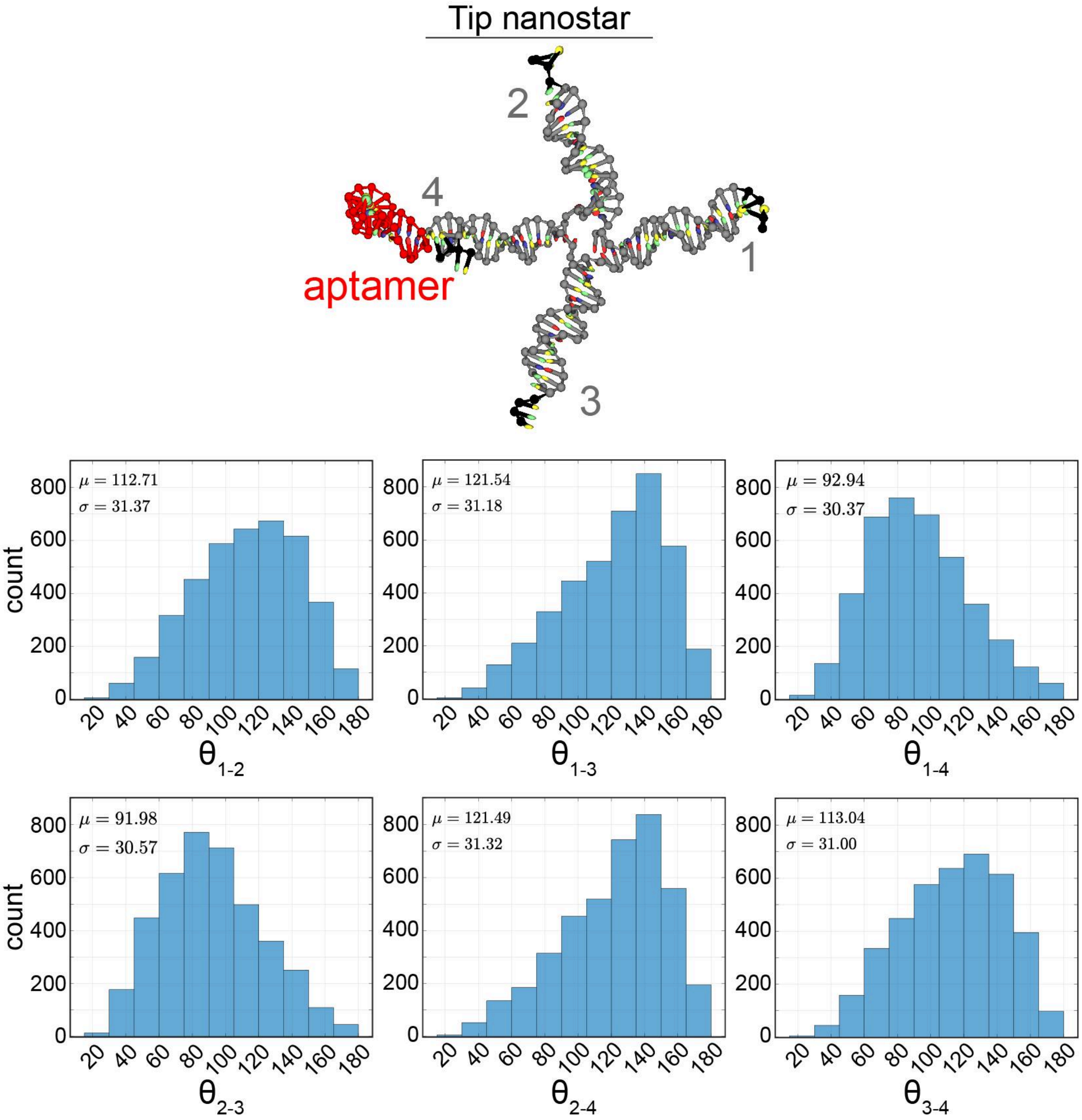

Figure S11. Angular distribution of the tip design. *Angular distributions of each and every pair of arms in the tip design. The i and j indices refer to the arm labels shown in the oxView representation (top).*

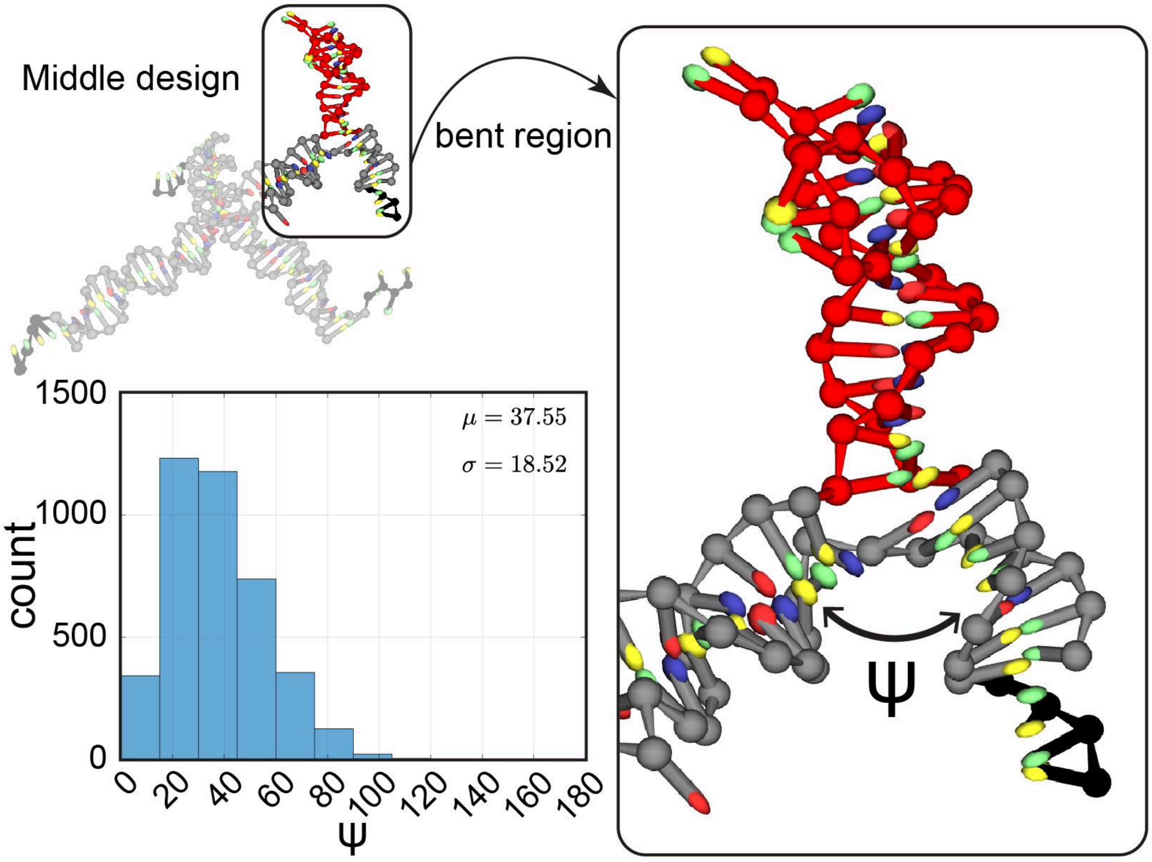

Figure S12. Arm bending caused by the aptamer presence in the middle of an arm. *The presence of the aptamer in the middle of the arm leads to an acute average with a sharp peak for the angle between the two segments of the arm.*

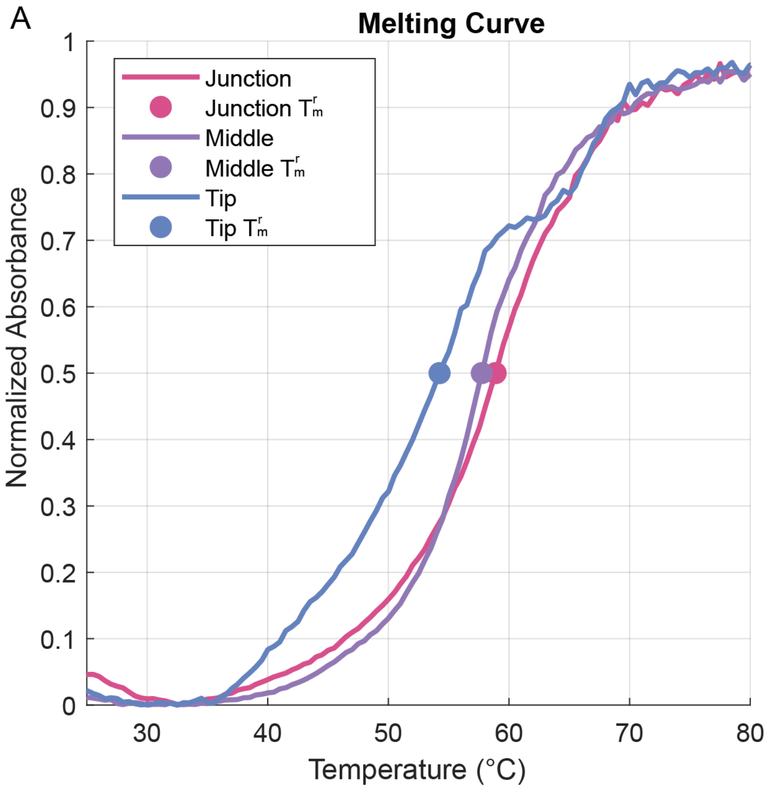

Figure S13. Melting behavior of the system. *Melting curves were measured for each nanostar design by raising the temperature from 25 °C to 80 °C and measuring absorbance. Junction crosses y = 0.5 at 58.9 °C, middle crosses y = 0.5 at 57.8 °C, and tip crosses y = 0.5 at 54.2 °C (n=1).*

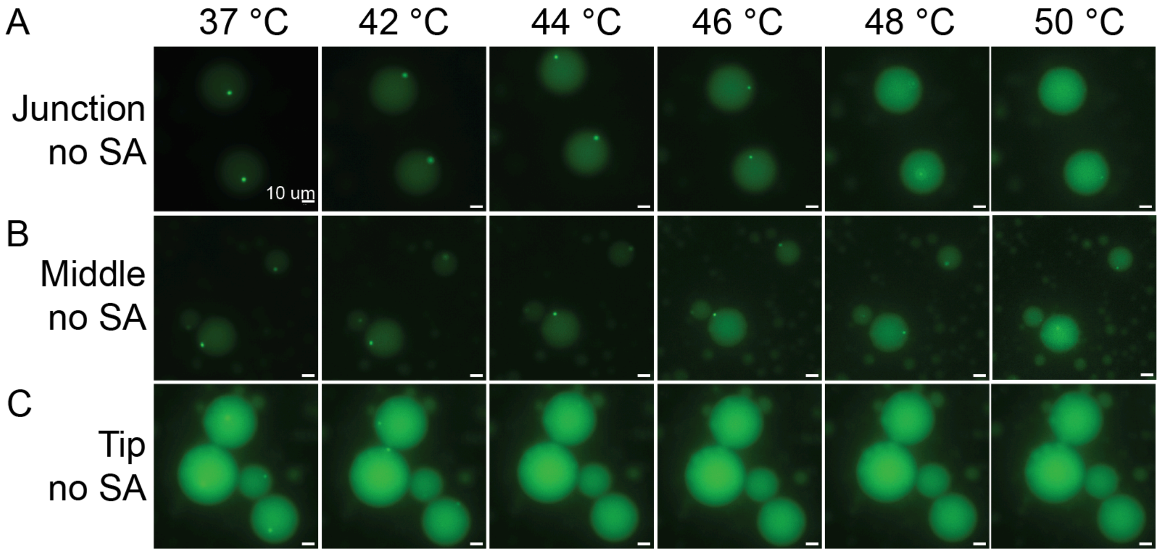

Figure S14. Condensates melting behavior in confinement. *Additional example epifluorescence microscopy images of condensates in emulsions droplets without SA, imaged from 37 ° C to 50 ° C for (A) junction, (B) middle, and (C) tip designs.*

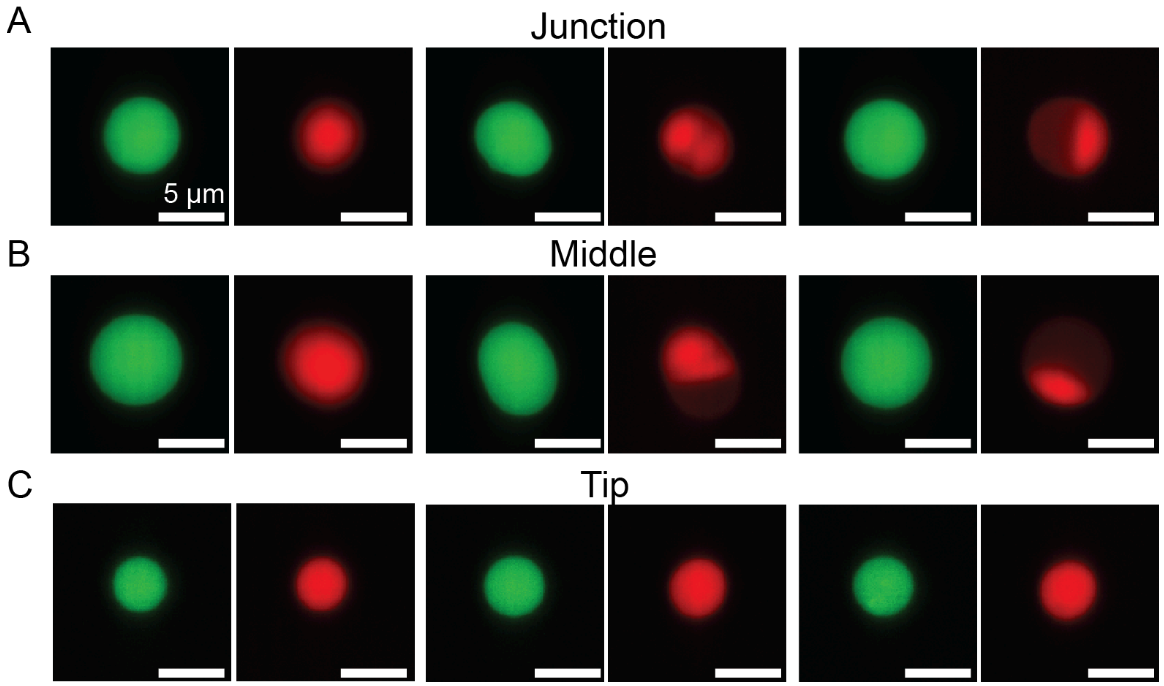

Figure S15. Incomplete protein release at low kleptamer concentrations. *Confocal images of separate channels corresponding to Figure 5B for 0.5x kleptamer strand, where green is the nanostar (FAM) and red is the SA (Alexa 647). Images were taken 60 minutes after kleptamer addition for (A) junction, B) middle, and (C) tip designs.*

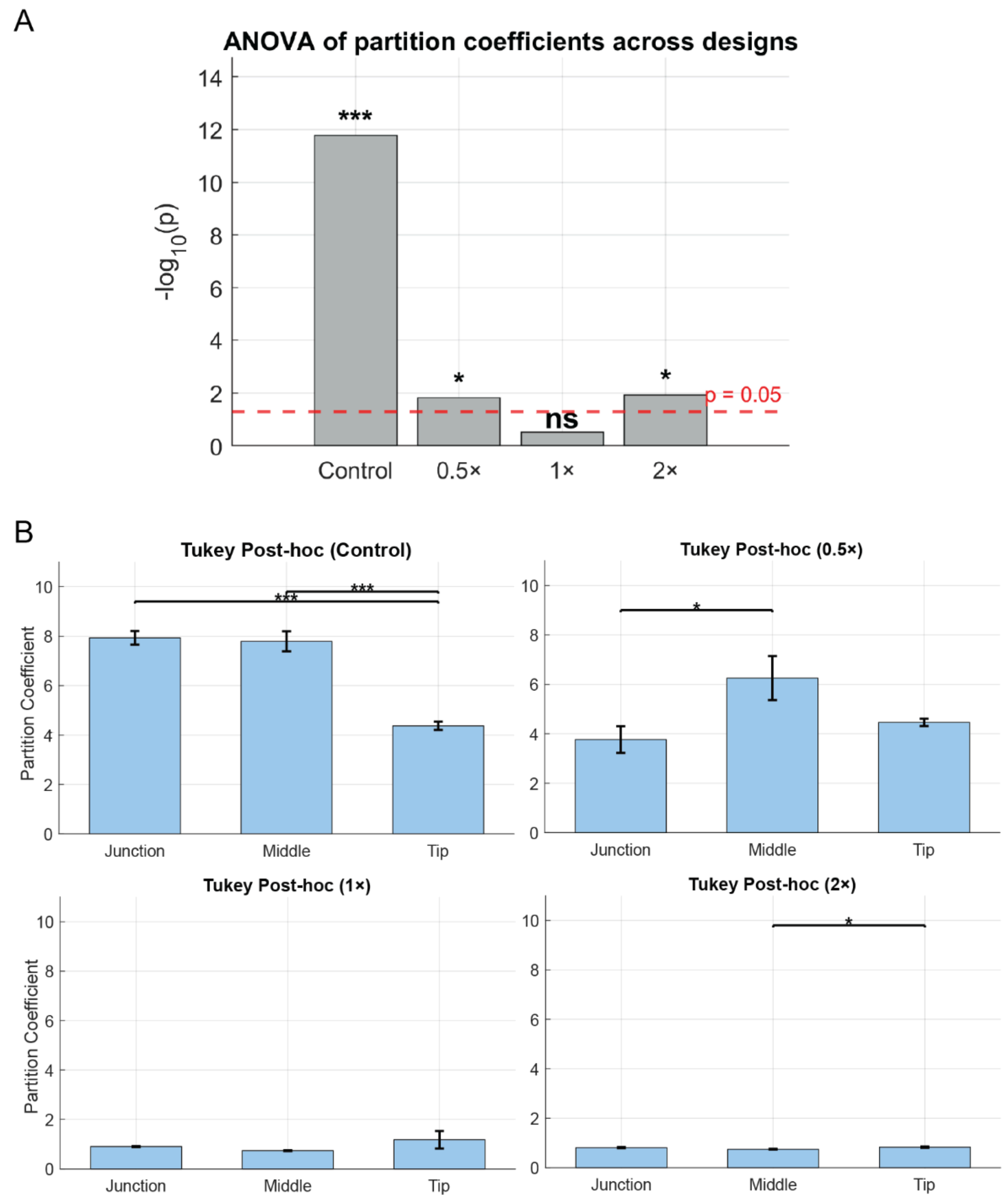

Figure S16. Statistical significant analysis of protein release across the designs. *(A) Global spatial heterogeneity across conditions. The bars represent -log10(p) values obtained from one-way ANOVA comparing junction, middle, and tip designs among kleptamer conditions. Dashed line indicates p = 0.05 significance threshold; asterisk denotes ANOVA significance (*p < 0.05, **p < 0.01, ***p< 0.001); "ns" denotes not significant. (B) Tukey post-hoc graphs show where significant differences in partition coefficients arise between designs at different kleptamer concentrations.*

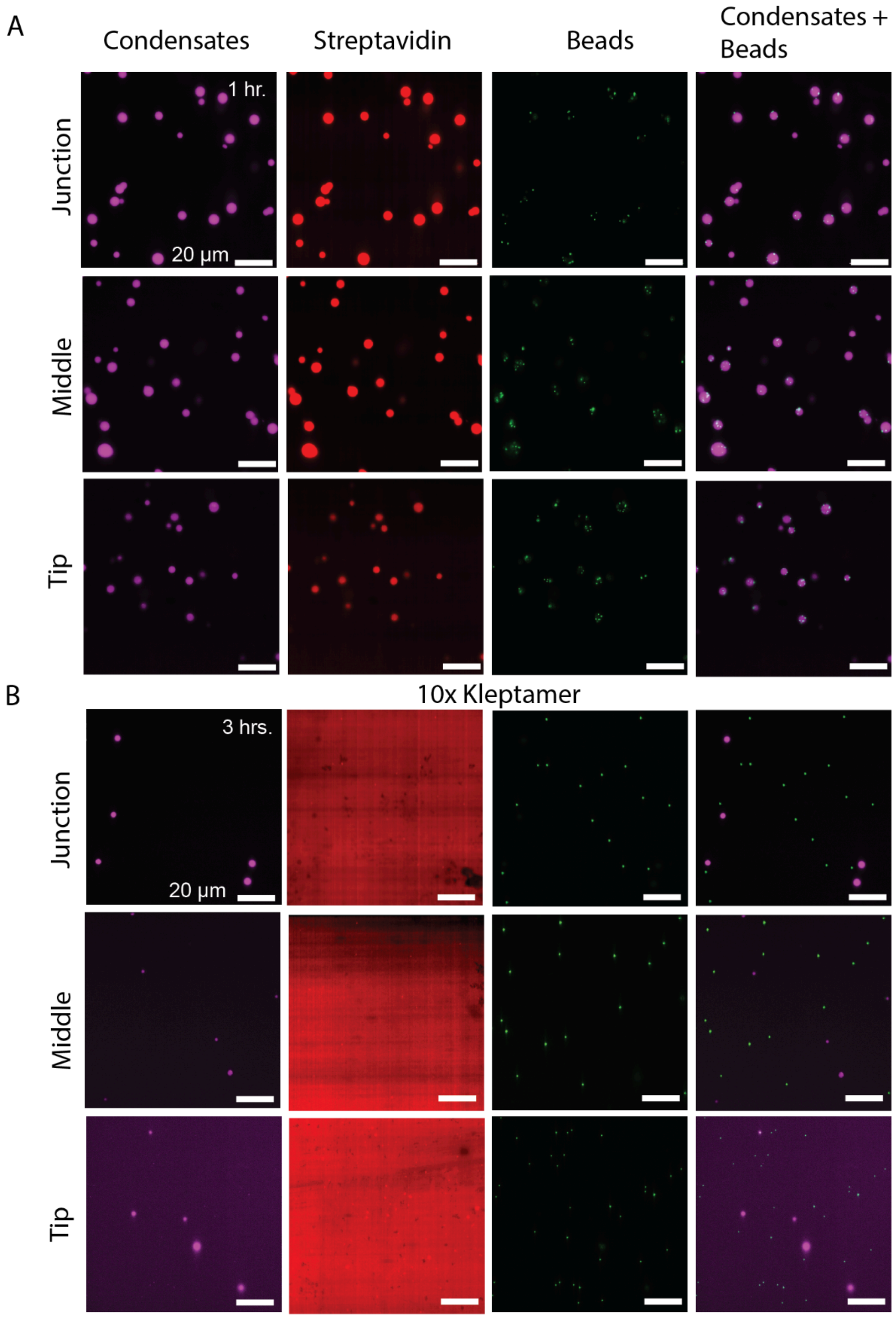

Figure S17. Beads recruitment and release via SA-containing condensates. *Confocal images of individual channels show condensates, streptavidin, beads, and a composite image of beads + condensates (A) before and (B) after kleptamer addition. Droplet size decreases 3 hours after kleptamer addition (4 hours post-anneal). The reduction may result from dilution, as well as sedimentation, which has been previously observed in samples incubated for longer than 3 hours[2].*

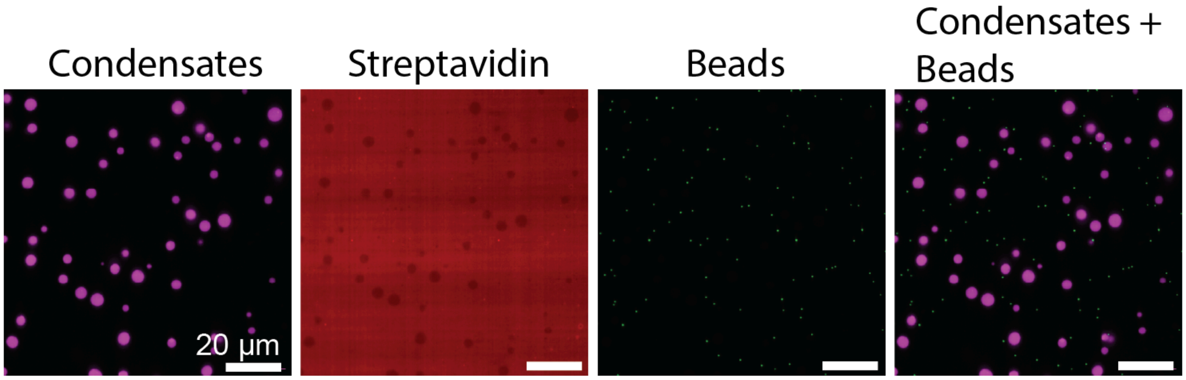

Figure S18. SA recruitment is essential for beads uptake. *At 350 mM NaCl, the control shows that recruitment of SA and beads does not occur when using nanostars (valency 4) without a DNA aptamer.*

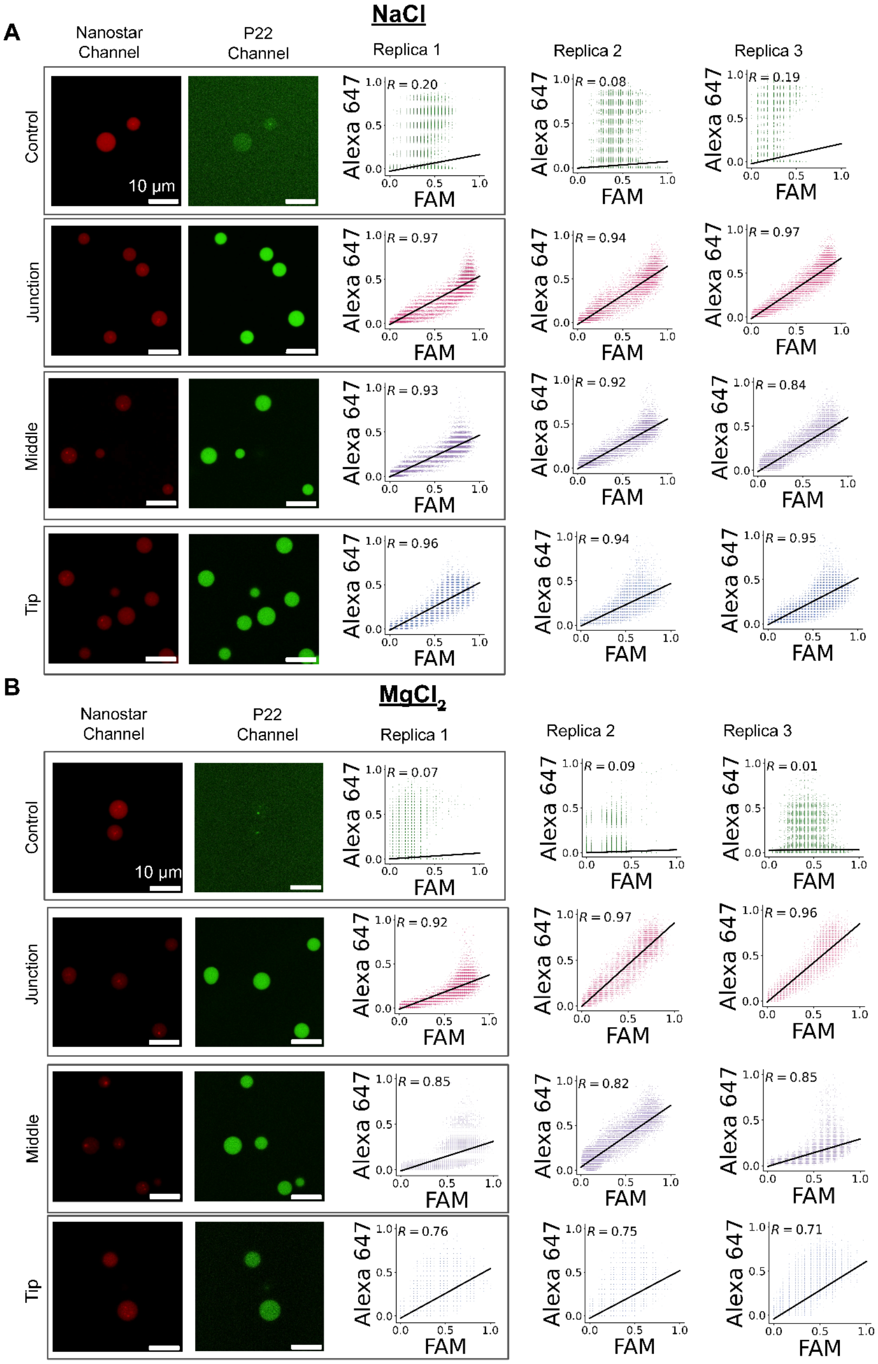

Figure S19. Recruitment of P22 protein using hybrid nanostars with RNA aptamer (BoxB). *Pearson's correlation coefficient for the recruitment of P22 using hybrid DNA-RNA condensates. Two different buffers were used: (A) NaCl, and (B) MgCl2. As a negative control, 4-arm, all-DNA nanostars without an aptamer were used to assess non-specific colocalization of P22 and condensates. All the experiments for control, junction, middle, and tip designs were done in triplicate (n = 3). It should be noted that P22 exhibited weak, non-specific colocalization with condensates in some instances, more notably with NaCl.*

2. Supplementary tables

Table S1. *DNA strands used in this study to form the core of the three proposed designs: junction, middle, and tip designs*[2,3].

Oligonucleotide strand name	**5’-Sequence-3’**
S1	GCGC**CAGTGAGGACGGAAGT**TT**GTCGTAGCATCGCACC**
S2	GCGC**CAACCACGCCTGTCCA**TT**ACTTCCGTCCTCACTG**
S3	GCGC**CCATGGTCCCAAGTGA**TT**TGGACAGGCGTGGTTG**
S1$^{\text{fam}}$	/**fam**/**CAGTGAGGACGGAAG**TT**TGTCGTAGCATCGCACC**
S1$^{\text{atto647}}$	/**atto647**/**CAGTGAGGACGGAAG**TT**TGTCGTAGCATCGCACC**

Table S2. *This table provides P22 peptide sequence; oligonucleotide sequences of strand S4 of the nanostar, which incorporates the aptamer domain for SA in different placements[4]; as well as the gene sequences for the RNA strands with P22 aptamer, i.e., BoxB[5]. Red bases represent the SA aptamer sequence, taken from the literature[4]. Purple bases indicate 'GC' pairs added to stabilize the stem of the aptamer to ensure correct folding. Only one 'GC' pair was added for the tip aptamer strand, which is sufficient to achieve its desired secondary structure without unwanted binding to the adjacent sticky end. The kleptamer strand has 28 complementary nucleotides to the aptamer domain, excluding 5 base pairs for the middle and junction designs and 3 base pairs for the tip design, to minimize the secondary structure of the kleptamer with aptamer (see also Table S7 for NUPACK binding prediction between aptamer and kleptamer). The polyT strand (28-nt long) was used to assess the binding specificity of the kleptamer strand.*

Oligonucleotide strand name	**5'-Sequence-3'**
junctionApt_S4_4_16	GCGCGGTGCGATGCTACGACGCATTGACCGCTGTGTGACGCAACACTCAATGCTCACTTGGGACCATGG
middleApt_S4_4_16	GCGCGGTGCGAGCATTGACCGCTGTGTGACGCAACACTCAATGCGCTACGACTTTCACTTGGGACCATGG
tipApt_S4_4_16	GCGCGGTGCGATGCTACGACTTTCACTTGGGACCATGGCATTGACCGCTGTGTGACGCAACACTCAATG
kleptamer	TTGAGTGTTGCGTCACACAGCGGTCAAT
polyT	TTTTTTTTTTTTTTTTTTTTTTTTTTTT
junctionApt_P22_S4_4_16	GCGCGGUGCGAUGCUACGACGCGGUGCGCUGACAAAGCGCGCCGCUCACUUGGGACCAUGG
middleApt_P22_S4_4_16	GCGCGGUGCGAGCGGUGCGCUGACAAAGCGCGCCGCGCUACGACUUUCACUUGGGACCAUGG
tipApt_P22_S4_4_16	GCGCGGUGCGAUGCUACGACUUUCACUUGGGACCAUGGuGGUGCGCUGACAAAGCGCGCC
NT_junction_BoxB_S4	GTACGTAATACGACTCACTATAGCGCGGTGCGATGCTACGACGCGGTGCGCTGACAAAGCGCGCCGCTCACTTGGGACCATGG
T_junction_BoxB_S4	CCATGGTCCCAAGTGAGCGGCGCGCTTTGTCAGCGCACCGCGTCGTAGCATCGCACCGCGCTATAGTGAGTCGTATTACGTAC
NT_middle_BoxB_S4	GTACGTAATACGACTCACTATAGCGCGGTGCGAGCGGTGCGCTGACAAAGCGCGCCGCGCTACGACTTTCACTTGGGACCATGG

T_middle_BoxB_S4	CCATGGTCCCAAGTGAAAGTCGTAGCGCGGCGCGCTTTGTCAGCGCACCGCTCGCACCGCGCTATAGTGAGTCGTATTACGTAC
NT_tip_BoxB_S4	GTACGTAATACGACTCACTATAGCGCGGTGCGATGCTACGACTTTCACTTGGGACCATGGtGGTGCGCTGACAAAGCGCGCC
T_tip_BoxB_S4	GGCGCGCTTTGTCAGCGCACCaCCATGGTCCCAAGTGAAAGTCGTAGCATCGCACCGCGCTATAGTGAGTCGTATTACGTAC
P22 N peptide sequence	GNAKTRRHERRRKLAIERDTIGY

***Table S3**. NUPACK analysis of the nanostars with the junction, middle, and tip aptamer placements.*

Junction nanostar

MFE proxy structure at 37°C

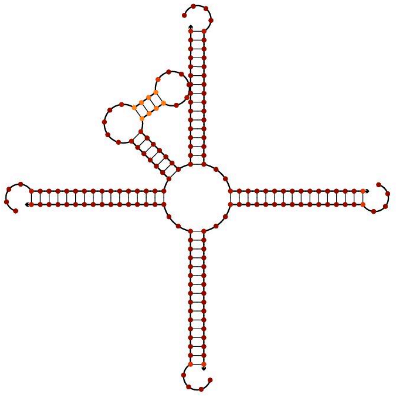

Free energy of the secondary structure: -99.35 kcal/mol

Equilibrium base-pairing probabilities at 37 ºC

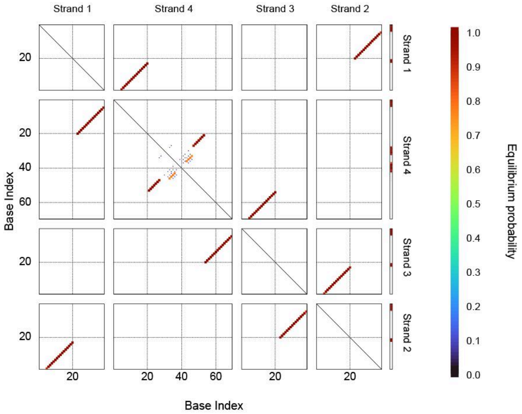

Free energy of complex (-kT log Q): -100.03 kcal/mol

Middle nanostar

MFE proxy structure at 37°C

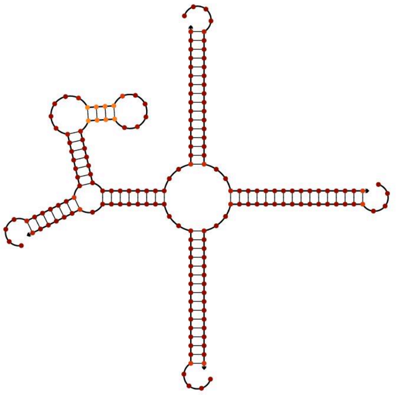

Free energy of the secondary structure: -93.05 kcal/mol

Equilibrium base-pairing probabilities at 37 ºC

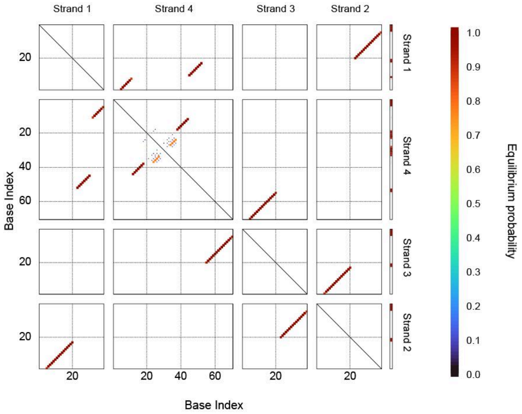

Free energy of complex (-kT log Q): -93.89 kcal/mol

Tip nanostar

MFE proxy structure at 37°C

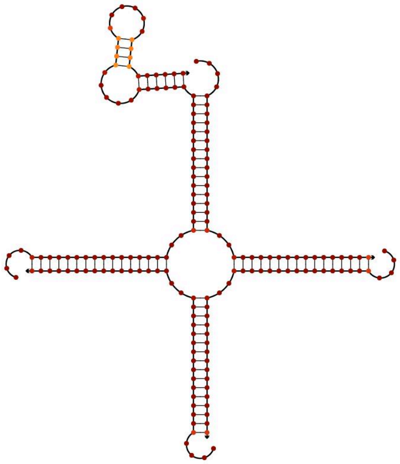

Equilibrium base-pairing probabilities at 37 ºC

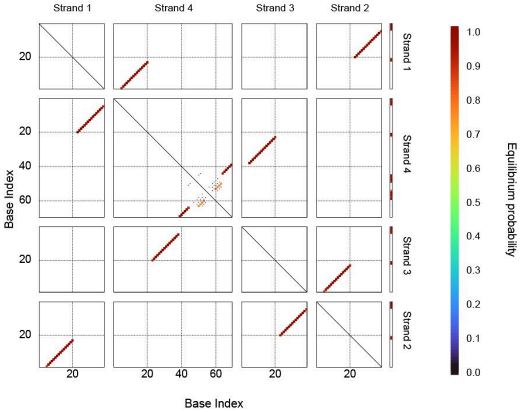

Free energy of complex (-kT log Q): -99.34 kcal/mol

Free energy of the secondary structure: -98.65 kcal/mol

Table S4. *Growth Curve Parameters corresponding to the condensation of each nanostar design in the presence of SA.*

$y = gt^{\alpha}$		**25℃**		**37℃**	
		g	α	***g***	α
2.5 μM	Junction	**0.48788**	**0.81882**	**1.72890**	**0.38170**
	Middle	**0.36727**	**0.82245**	**1.71440**	**0.42147**
	Tip	**0.67913**	**0.58128**	**0.73283**	**0.42952**
1.25 μM	Junction	**1.17820**	**0.28627**	**0.93790**	**0.41758**
	Middle	**0.86944**	**0.40197**	**0.62066**	**0.50532**
	Tip	**1.28240**	**0.24577**	**0.96884**	**0.22124**

Table S5. *Growth Curve Parameters corresponding to the condensation of each nanostar design in the absence of SA.*

$y = gt^{\alpha}$		**25℃**		**37℃**	
		g	α	***g***	α
2.5 μM	Junction	**0.15554**	**1.2075**	**0.53488**	**0.67758**
	Middle	**0.29593**	**0.94732**	**1.25940**	**0.48670**
	Tip	**0.24542**	**0.97941**	**1.4471**	**0.14999**
1.25 μM	Junction	**0.33875**	**0.83748**	**2.26350**	**0.14961**
	Middle	**0.90454**	**0.41016**	**0.69771**	**0.49366**
	Tip	**1.2599**	**0.26987**	**1.2049**	**0.19467**

Table S6. *Parameters used in the oxDNA simulations.*

MC relaxation

```
backend = CPU
backend_precision = double

max_backbone_force = 5
max_backbone_force_far = 10

interaction_type = DNA2

ensemble = NVT

delta_translation = 0.22
delta_rotation = 0.22
verlet_skin = 1.0
cells_auto_optimisation = true

sim_type = MC
steps = 500000

T = 290K
salt_concentration = 1

refresh_vel = true

use_average_seq = 1
```

MD relaxation

```
backend = CPU
backend_precision = double

max_backbone_force = 5
max_backbone_force_far = 10

interaction_type = DNA2

CUDA_list = verlet
CUDA_sort_every = 0

use_edge = 1
edge_n_forces = 1
max_density_multiplier = 10
verlet_skin = 1.0
cells_auto_optimisation = true

sim_type = MD
steps = 500000

T = 290K
salt_concentration = 1

dt = 0.0001
thermostat = langevin
diff_coeff = 0.5
newtonian_steps = 103

reset_com_momentum = true
refresh_vel = true

use_average_seq = 1
```

MD simulation

```
####
####  PROGRAM PARAMETERS
####
interaction_type = DNA2
sim_type = MD
backend = CPU
backend_precision = double
debug = 1

####
####    SIM PARAMETERS
####
steps = 200000000
newtonian_steps = 103
diff_coeff = 2.50
thermostat = john

list_type = cells
ensemble = nvt
delta_translation = 0.22
delta_rotation = 0.22

T = 37C
salt_concentration = 1.0
dt = 0.003
verlet_skin = 0.5

max_backbone_force = 5
```

Table S7*. NUPACK prediction of kleptamer and aptamer binding.*

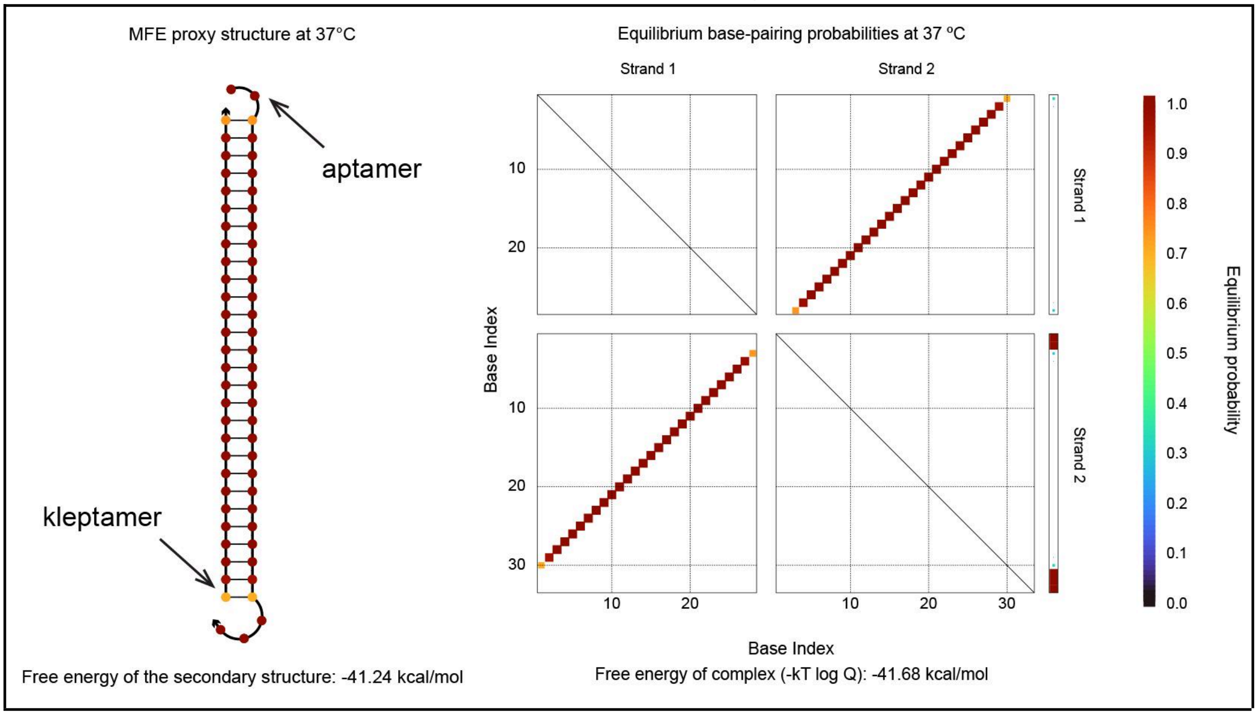

MFE proxy structure at 37°C

Equilibrium base-pairing probabilities at 37 ºC

Free energy of the secondary structure: -41.24 kcal/mol

Free energy of complex (-kT log Q): -41.68 kcal/mol

Table S8. *One-way ANOVA p-values and Tukey post-hoc comparisons for junction, middle, and tip designs across different kleptamer concentrations.*

Condition	ANOVA p-value	Junction vs. Middle	Junction vs. Tip	Middle vs. Tip
Control	1.638e-12	9.398e-01	4.277e-11	1.539e-10
0.5x	1.561e-02	1.440e-02	6.977e-01	1.011e-01
1x	3.108e-01	8.367e-01	6.058e-01	2.855e-01
2x	1.217e-02	6.420e-02	8.000e-01	1.310e-02

3. References

1 S. Agarwal, D. Osmanovic, M. A. Klocke and E. Franco, *ACS Nano*, 2022, **16**, 11842–11851.

2 S. Agarwal, D. Osmanovic, M. Dizani, M. A. Klocke and E. Franco, *Nat Commun*, 2024, **15**, 1915.

3 M. Dizani, D. Sorrentino, S. Agarwal, J. M. Stewart and E. Franco, *J Am Chem Soc*, 2024, **146**, 29344–29354.

4 T. Bing, X. Yang, H. Mei, Z. Cao and D. Shangguan, *Bioorg Med Chem*, 2010, **18**, 1798–1805.

5 T. S. Bayer, L. N. Booth, S. M. Knudsen and A. D. Ellington, *RNA*, 2005, **11**, 1848–1857.